How to cite: *Angew. Chem. Int. Ed.* **2024**, e202406909
doi.org/10.1002/anie.202406909

Metal-Organic Cages

Metal Ions Trigger the Gelation of Cysteine-Containing Peptide-Appended Coordination Cages

Meng Li, Huangtianzhi Zhu, Simone Adorinni, Weichao Xue, Andrew Heard, Ana M. Garcia, Slavko Kralj, Jonathan R. Nitschke, and Silvia Marchesan**

Abstract: We report a series of coordination cages that incorporate peptide chains at their vertices, prepared through subcomponent self-assembly. Three distinct heterochiral tripeptide subcomponents were incorporated, each exhibiting an L–D–L stereoconfiguration. Through this approach, we prepared and characterized three tetrahedral metal-peptide cages that incorporate thiol and methylthio groups. The gelation of these cages was probed through the binding of additional metal ions, with the metal-peptide cages acting as junctions, owing to the presence of sulfur atoms on the peripheral peptides. Gels were obtained with cages bearing cysteine at the C-terminus. Our strategy for developing functional metal-coordinated supramolecular gels with a modular design may result in the development of materials useful for chemical separations or drug delivery.

The encounter between cages and gels gives rise to the formation of novel nanomaterials, with potential for applications based upon the hierarchical structures that emerge from cage-gel hybrid systems.[1] Metal-organic cages with well-defined cavities have proven useful for applications that include chemical purification,[2] drug delivery,[3] catalysis,[4] sensing[5] and the modulation of photophysical properties.[6] The combination of gels with cages can enable the development of smart materials that respond to external stimuli,[7] for instance, disassembling and reforming,[8] or converting energy from one form into another,[9] while being recyclable.[10] Two methods have been shown to enable the connection of metal-organic cages to form cage-gel materials. The first involves non-covalent interactions to link cages,[11] while the second employs covalent linking through polymer chains.[12] The use of peptides to join cages non-covalently is of particular interest, since peptides are readily accessible and the resulting materials can be designed to be adaptive and biocompatible.[13]

Previous work prepared supramolecular gels by embedding cages into peptide gels in acetonitrile.[14] Tripeptides featuring hydrophobic amino acids with L–D–L stereochemistry have been shown to adopt an amphipathic conformation that enables their self-organization into gelling fibers.[15] These precedents enabled us to hypothesize that the incorporation of short, structured peptides into cages could yield a new class of cage-gels. This strategy could thus enable the modular design of new porous gels with properties tailored for specific functions.

Metal-coordination-driven assembly of peptides offers a platform for the creation of multifunctional supramolecular materials.[16] Metal-binding natural amino acids, such as histidine (His), cysteine (Cys), and methionine (Met) have been incorporated into synthetic ligands to explore new routes to the design of structured supramolecular assemblies from short peptides.[17] This study presents a strategy for the design of cage-gels that form upon metal-triggered crosslinking of the peripheral peptide arms of metal-organic cages.

We chose ligands bearing either Cys or Met and aminobenzoyl units (Figure 1a). The *p*-aminobenzoyl moiety incorporated into the cage vertices following metal-ion templated imine condensation, while the Cys or Met residues on the pendant peptides could serve to crosslink cages into gel-forming networks upon binding a second metal ion.[18] The reaction of 5,5′,5″-(benzene-1,3,5-triyl)tripicolinaldehyde (**A**, 4 equiv.) with (*p*-aminobenzoyl)-L–Phe–D–Cys–L–Phe–NH_2 (**B**, 12 equiv.) and iron (II) bis(trifluoromethanesulfonyl)imide ($Fe^{II}(NTf_2)_2$, 4 equiv.) in CH_3CN at 343 K produced cage **1** (Figure 1b). Its $Fe^{II}{}_4L_4$

[*] Dr. M. Li
Department of Environmental Science and Engineering, North China Electric Power University
689 Huadian Road, Baoding 071003, P. R. China

Dr. M. Li, Dr. H. Zhu, Dr. W. Xue, Dr. A. Heard, Prof. J. R. Nitschke
Department of Chemistry, University of Cambridge
Lensfield Road, Cambridge, CB2 1EW, UK
E-mail: jrn34@cam.ac.uk

Dr. M. Li, Dr. S. Adorinni, Dr. A. M. Garcia, Prof. S. Marchesan
Department of Chemical & Pharmaceutical Sciences
University of Trieste, Via L. Giorgieri 1, 34127 Trieste, Italy
E-mail: smarchesan@units.it

Dr. S. Kralj
Materials Synthesis Department, Jožef Stefan Institute
Jamova 39, 1000 Ljubljana, Slovenia

Dr. S. Kralj
Pharmaceutical Technology Department – Faculty of Pharmacy, University of Ljubljana,
Aškerčeva 7, 1000 Ljubljana, Slovenia

Prof. S. Marchesan
INSTM, Unit of Trieste
34127 Trieste, Italy

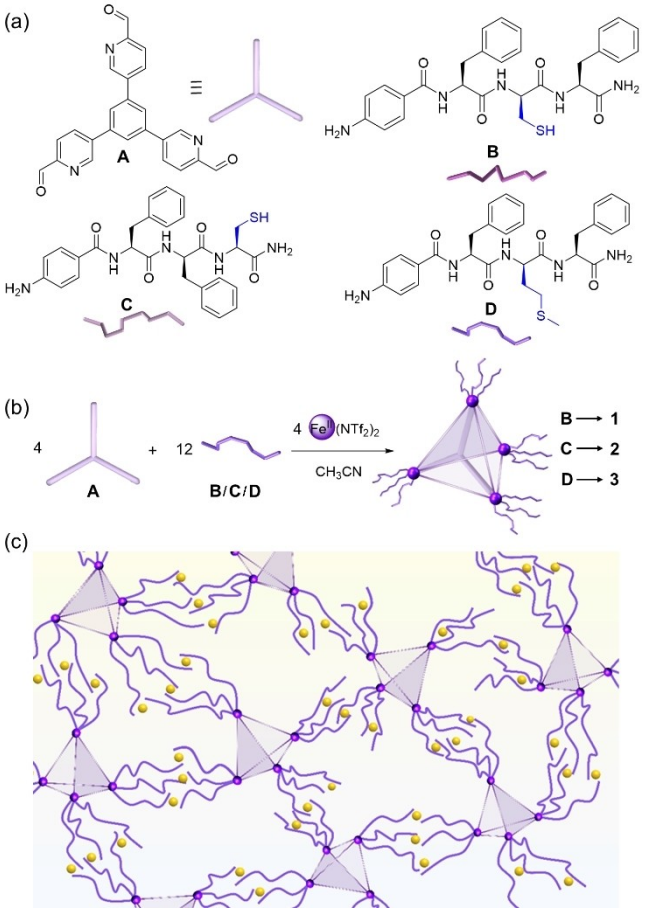

Figure 1. (a) Chemical structures and schematic representations of the tris(formylpyridine) (**A**) and aniline-terminated tripeptide subcomponents (**B**–**D**). (b) The subcomponent self-assembly of $Fe^{II}_4L_4$ tetrahedra **1**–**3**. (c) Cages **1**–**3** were probed for gelation upon addition of a second metal (yellow sphere) for coordination with the sulfur-bearing peptides).

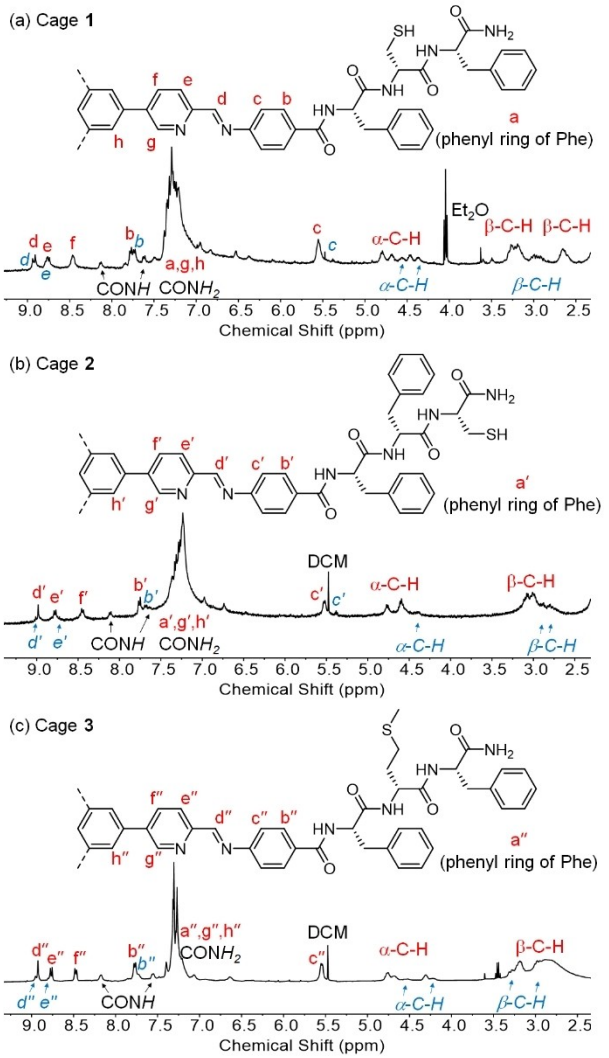

Figure 2. Partial ^{1}H and DOSY NMR spectra of cages (a) **1**, (b) **2**, and (c) **3** (CD_3CN, 400 MHz, 298 K), showing the aromatic and the peptide regions. Red letters correspond to peaks assigned to the major diastereomer Λ_4 while blue italic letters correspond to the minor diastereomer Δ_4. DCM = dichloromethane.

composition was confirmed by high-resolution electrospray ionization mass spectrometry (Figures S21–S22). The incorporation of (*p*-aminobenzoyl)-L–Phe–D–Phe–L–Cys–NH_2 (**C**) and (*p*-aminobenzoyl)-L–Phe–D–Met–L–Phe–NH_2 (**D**) was also investigated, giving rise to tetrahedral cages **2** and **3** (Figures S28–S29 and S39–S40), respectively.

The ^{1}H NMR and diffusion-ordered spectroscopy (DOSY) spectra of cages **1**–**3** are reported in Figure 2 (see ESI, Section 2). The limited solubility of cages **1**–**2** did not allow for the acquisition of ^{13}C NMR spectra, although ^{1}H NMR and DOSY (Figures 2a–b and S17, S19, S23, S25) confirmed successful cage formation, with the appearance of the typical signals above 8.5 ppm (absent in the parent peptides) from imine condensation and iron coordination at the cage vertices. In both cases, DOSY analyses revealed the presence of solely one species, with diffusion coefficients corresponding to solvodynamic radii of approximately 2 and 3 nm, respectively, compatible with the expected cage dimensions. Cage **3**, having longer alkyl chains and higher solubility, enabled a more detailed structural characterization by ^{1}H and 2D NMR (Figures 2c and S30–S38), with two sets of proton signals in a ratio of 2.5:1, with the same diffusion coefficient observed for both sets of peaks in the DOSY spectrum, corresponding to a radius of 2 nm (Figure S34). This observation indicates that **3** exists as a pair of diastereomers with opposite handedness at its Fe^{II} vertices: Δ_4-**3** and Λ_4-**3**.[19] We infer the diastereomeric enrichment of **3** to be a consequence of stereochemical information transfer from the enantiopure peptide side chains to the metal vertices during self-assembly.[20] A lower level of stereocontrol was found for cages **1**–**2**, and especially for **1**, as evidenced by the complexity of the NMR signals of the peptide α protons (Figure 2a). Indeed, cage **1** integrates peptide **B**, which is the least sterically hindered at the second amino acid (while the first one is Phe in all cases).

To identify the major diastereomer, circular dichroism (CD) analysis of **3** was conducted. The CD spectrum of **3** displayed clear Cotton effects at 210–410 nm and 490–

630 nm, corresponding to π–π* and metal-to-ligand charge transfer (MLCT) transitions, respectively (Figure S44). The observed sign of the MLCT bands corresponds to *Λ*-handedness of the metal vertices.[21] We therefore infer the major diastereomer of **3** to be Λ_4-**3**, and the minor diastereomer, Δ_4-**3**. Cages **1** and **2** also formed with predominant Λ_4 stereochemistry but with lower diastereoselectivity (Figures S44). As expected, the opposite result is obtained using a peptide enantiomer, as demonstrated by a mirror-image CD spectrum (Figure S45). Although the stereochemical information transfer observed here is moderate, our work may provide an insight into using homochiral peptides, which contain chiral directing groups far from the coordination sites, to control cage stereochemistry.[22]

We then examined the gelation of cages **1**–**3** by performing tube inversion tests. No gels were observed to form from saturated cage solutions (ca. 5 mM) or through the oxidation of the Cys residues to form disulfide crosslinks, which can induce peptide assembly and gelation (Table S1).[23]

Cys thiols can also coordinate metal ions. Cages **1** and **2** were thus tested for metal-coordination-driven gelation (Table S2). Upon the addition of an acetonitrile solution of AgOTf to the solution of **1**, gels were not observed even at $[Ag^+] = 90$ mM; nor were Zn^{2+} or Hg^{2+} observed to induce gelation at these concentrations. We infer that the thiol groups may be too close to the hindered cage vertices to allow for metal-ion-induced cage crosslinking to form gels. Likewise, even though Met sulfur can coordinate metals, no gels were obtained from cage **3**.

In contrast, the thiol group on **2** is located farther from the cage core, in a potentially more accessible position. Upon treatment of a solution of cage **2** with AgOTf in acetonitrile, followed by two minutes of sonication, the transformation of the purple solution of cage **2** into a purple metallogel was observed (Figure 3a). Zn^{2+} and Hg^{2+} were likewise observed to trigger gelation, as demonstrated by tube inversion tests (Figure 3e, 3i).

The ability of solely cage **2** to gel upon coordination with metals could be the result of peptide conformation too, which could explain the larger solvodynamic radius of cage **2**, relative to cages **1** and **3**, derived from DOSY data. Notably, the near-UV region of the CD spectrum of cage **2**,

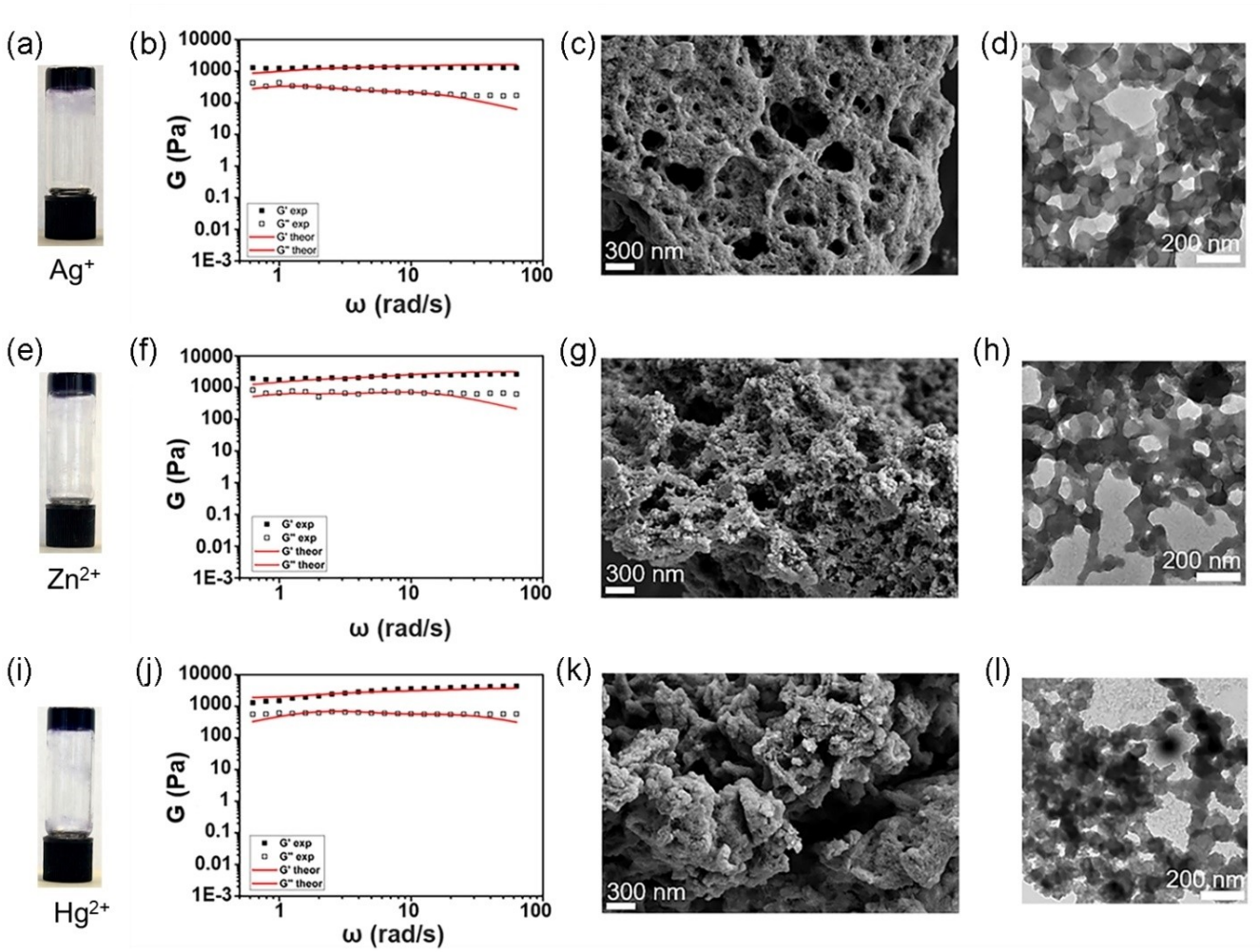

Figure 3. Photographs, rheology (frequency sweeps), SEM and TEM images of gels of cage **2** triggered by (a–d) Ag^+, (e–h) Zn^{2+}, (i–l) Hg^{2+}, respectively. Red lines in (a), (d), and (g) indicate the fittings (Maxwell)[33] to derive the elastic (G′) and viscous (G″) moduli of the hydrogels.

where pepide conformations are associated with distinctive signatures, was different from those of cages **1** and **3**, analogously to the situation found for the CD spectra of the parent peptides. Indeed, peptides **B** ((*p*-aminobenzoyl)-L–Phe–D–Cys–L–Phe–NH_2) and **D** ((*p*-aminobenzoyl)-L–Phe–D–Met–L–Phe–NH_2) leading to non-gelling cages **1** and **3**, respectively, displayed the characteristic signals of hydrophobic, self-assembling L–Phe–D–Xaa–L–Phe (Xaa = hydrophobic, aliphatic aa) peptides that were assigned to β-structures.[15a] In contrast, peptide **C** ((*p*-aminobenzoyl)-L–Phe–D–Phe–L–Cys–NH_2) leading to gelling cage **2** displayed a peculiar CD signature that was reminiscent of those ascribed to polyproline II helices (PPII)[24] or the similar type-I turns.[25] PPII conformers are attractive building blocks for assemblies that rely on coordination to precious metals,[26] while turns are highly sought after because they are often found in bioactive motifs.[27] Tripeptides are too short to satisfy the classification requirements of these types of conformations[28] that have been reported for sequences bearing at least four residues.[29] However, there is a recent example of a gelling tripeptide featuring the Phe-Phe motif and a similar CD spectrum upon assembly.[30] It is worth noting that the CD spectrum of peptide **C** was characterised by a distinctive Cotton effect, with a positive maximum at 254 nm and a negative minimum at 228 nm, indicating a positive exciton coupling, which manifests when two interacting units display the long axes so as to constitute a clockwise screw sense.[31] The effects of metal binding on the peptide conformation were studied by UV/Vis and CD on cage **2**, yet no changes were observed due to the predominant strong signals of the aromatic panels of the cage. Peptide **C** alone could not be used as a model for cage **2** due to the presence of the free *p*-aminophenyl moiety that coordinated the metals along with the Cys thiol (Figure S6). The N-acetylated analog to peptide **C** was thus studied as a model, although in this case the turn conformation was lost in favor of β-structures, as confirmed by CD spectra (Figures S46–S48). Nevertheless, the spectroscopic evolution upon metal coordination confirmed the occurrence of chemically triggered conformational changes, as reported for a tripeptide in a MOF.[32] In both cases, the observed effects enabled changes in the resulting functional materials (i.e., gels in our case).

The viscoelastic properties of the cage-gels were studied by oscillatory rheology. (Figures 3b,f,j and S49–S51).[34] Frequency sweeps indicated that both the elastic (G′) and the viscous (G″) moduli were independent of the applied frequency, and $G' > G''$, confirming the presence of weak gels ($G' \leq 10\,G''$). Gelation kinetics revealed a two-stage process with a lag phase, suggesting a longer nucleation process relative to gel matrix formation, especially for Ag^+. Calculation of gel stiffness (Table S3) yielded shear moduli of 1.6 kPa, 3.2 kPa, and 3.9 kPa for Ag^+, Zn^{2+}, Hg^{2+}, respectively. Stress sweeps confirmed gel breaking just above 20 Pa for Ag^+, and at nearly 70 Pa for Hg^{2+} and Zn^{2+}.

These results suggest that the cations Hg^{2+} and Zn^{2+} coordinate more strongly to the thiol groups of the terminal Cys residues than Ag^+,[35] thus providing more crosslinks. Scanning electron microscopy (SEM) and transmission electron microscopy (TEM) provided insights into the observed rheological differences from a morphological point of view. Contrary to gels arising from tripeptide stacks that yield a fibrillar network,[15a] also in the presence of embedded cages,[13] gels **1**–**3** displayed spherical nuclei interconnected in the gel matrix (Figures 3d,h,l). The nuclei displayed an average diameter of 84 ± 29 nm in the case of Ag^+, whereas the gels triggered by Zn^{2+} and Hg^{2+} exhibited smaller average diameters of 45 ± 13 nm and 31 ± 18 nm, respectively (Figure S52). This observation may help to explain the longer lag phase prior to gelation in the case of Ag^+, which incorporates larger nuclei. Raman analyses (Figure S53) further confirmed that the cage framework remained intact after gelation.

XPS analysis was used to confirm metal coordination in the gels. For all three gels, the Fe 2p peak at 709.01–710.07 eV supported the presence of Fe–N coordination linkages within the cages.[36] The peak at 717.54 eV was attributed to Fe^{3+}, indicating trace oxidization (Figure S54).[37] The Ag^+-triggered gel displayed an Ag $3d_{3/2}$ peak at 373.53 eV and an Ag $3d_{5/2}$ peak at 367.50 eV, matching the Ag^I signal in Ag_2S (Figure 4a).[38] The S $2p_{1/2}$ peak at 162.78 eV and S $2p_{3/2}$ peak at 161.50 eV match the reported S^{2-} values in Ag_2S. The peaks at 167.18 and 168.08 eV, assigned to S $2p_{1/2}$, both match the sulfur(VI) signals in Tf_2N^- (Figure 4b).[39] Both Zn^{2+}-triggered and Hg^{2+}-triggered gels show similar characteristics, confirming

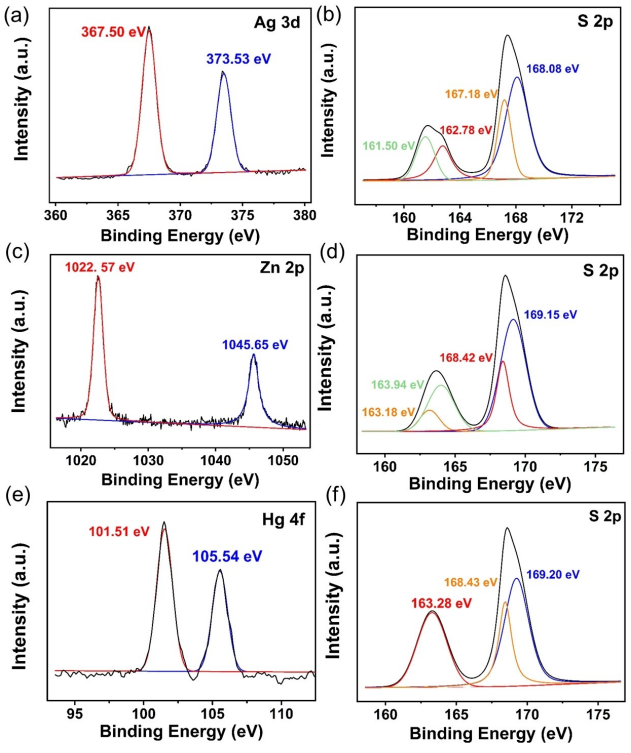

Figure 4. XPS analysis of three cage-peptide gels prepared from **2**. (a), (c) and (e) are XPS spectra corresponding to Ag 3d, Zn 2p, and Hg 4f, respectively, and (b) (d) and (f) are the S 2p XPS spectra for the same samples shown in (a), (c) and (e), confirming the presence of Tf_2N^- in each case.

the existence of Zn and Hg (Figure 4c–f, Figure S55).[40] All XPS data were consistent with the metal ions interacting with the thiol groups of the Cys residues incorporated into the peripheries of cages in gels.

The metal-organic cages we report here thus incorporate peptide subcomponents for the first time, the Cys residues of which are demonstrated to bind peripheral metal ions, bringing about gelation. The observed diastereoselectivity in cage formation reveals stereochemical information transfer from the peripheral arms to the metal vertices. This phenomenon showcases the ability to control the stereochemistry of the resulting cages by manipulating the stereochemistry of the peripheral arms, thereby opening a new pathway for the design of cages with controlled stereochemistry. The spherical nuclei formed during gelation interconnect to form a gel matrix, as opposed to the fibrillar networks observed for peptide gels. This gelation in the presence of heavy metals holds promise for the removal of toxic metal ions from the environment. Future efforts will focus upon the extension of this chemical platform to the formation of biocompatible materials able to perform catalysis and chemical purification by taking advantage of the two distinct spaces present within these gels—the voids within the cages, and the larger regions of trapped solvent immobilized by matrix formation.

Acknowledgements

The authors gratefully acknowledge funding from China Scholarship Council and M.L. acknowledges the ICTP-TRIL fellowship program. The visit of M.L. was supported by The Abdus Salam International Centre for Theoretical Physics (ICTP) based in Trieste, Italy, through its Programme for Training and Research in Italian Laboratories (TRIL). This project received funding from the European Union's Horizon 2020 research and innovation program under the Marie Sklodowska-Curie grant agreement No 642192 and was supported by the UK Engineering and Physical Sciences Research Council (EPSRC EP/P027067/1 and EP/T031603/1), the National Natural Science Foundation of China (No. 52370110) and the Fundamental Research Funds for the Central Universities (No. 2023MS146). This research was also funded by the Slovenian Research Agency (ARIS) through the core funding No. P2-0089, ARIS projects: No. J2-3043, J2-3040, J2-3046, J3-3079, J7-4420, and bilateral ARIS projects: BI-FR/23-24-PROTEUS-005 (PR-12039) and BI-RS/23-25-030 (PR-12782). The authors acknowledge the CEMM Nanocenter (JSI, Slovenia) for the access to electron microscopy.

Conflict of Interest

The authors declare no conflict of interest.

Data Availability Statement

The data that support the findings of this study are available from the corresponding authors upon reasonable request.

Keywords: self-assembly · metal-organic cages · supramolecular gel · peptides · chirality

[1] a) P. Sutar, T. K. Maji, *Chem. Commun.* **2016**, *52*, 8055–8074; b) W. Zheng, G. Yang, N. Shao, L.-J. Chen, B. Ou, S.-T. Jiang, G. Chen, H.-B. Yang, *J. Am. Chem. Soc.* **2017**, *139*, 13811–13820; c) N. Hosono, S. Kitagawa, *Acc. Chem. Res.* **2018**, *51*, 2437–2446; d) I. Jahovic, Y.-Q. Zou, S. Adorinni, J. R. Nitschke, S. Marchesan, *Matter* **2021**, *4*, 2123–2140; e) J. Liu, Z. Wang, P. Cheng, M. J. Zaworotko, Y. Chen, Z. Zhang, *Nat. Chem. Rev.* **2022**, *6*, 339–356; f) C. M. Brown, D. J. Lundberg, J. R. Lamb, I. Kevlishvili, D. Kleinschmidt, Y. S. Alfaraj, H. J. Kulik, M. F. Ottaviani, N. J. Oldenhuis, J. A. Johnson, *J. Am. Chem. Soc.* **2022**, *144*, 13276–13284.

[2] a) K. Wu, K. Li, Y.-J. Hou, M. Pan, L.-Y. Zhang, L. Chen, C.-Y. Su, *Nat. Commun.* **2016**, *7*, 10487; b) H. Zeng, X.-J. Xie, M. Xie, Y.-L. Huang, D. Luo, T. Wang, Y. Zhao, W. Lu, D. Li, *J. Am. Chem. Soc.* **2019**, *141*, 20390–20396; c) P.-F. Cui, Y.-J. Lin, Z.-H. Li, G.-X. Jin, *J. Am. Chem. Soc.* **2020**, *142*, 8532–8538; d) C. Garcia-Simon, A. Monferrer, M. Garcia-Borras, I. Imaz, D. Maspoch, M. Costas, X. Ribas, *Chem. Commun.* **2019**, *55*, 798–801.

[3] a) Y.-R. Zheng, K. Suntharalingam, T. C. Johnstone, S. J. Lippard, *Chem. Sci.* **2015**, *6*, 1189–1193; b) W. Zhu, J. Guo, Y. Ju, R. E. Serda, J. G. Croissant, J. Shang, E. Coker, J. O. Agola, Q.-Z. Zhong, Y. Ping, F. Caruso, C. J. Brinker, *Adv. Mater.* **2019**, *31*, 1806774.

[4] a) K. Wang, J. H. Jordan, X.-Y. Hu, L. Wang, *Angew. Chem. Int. Ed.* **2020**, *59*, 13712–13721; *Angew. Chem.* **2020**, *132*, 13816–13825; b) J. Koo, I. Kim, Y. Kim, D. Cho, I.-C. Hwang, R. D. Mukhopadhyay, H. Song, Y. H. Ko, A. Dhamija, H. Lee, W. Hwang, S. Kim, M.-H. Baik, K. Kim, *Chem* **2020**, *6*, 3374–3384; c) A. Dhamija, A. Gunnam, X. Yu, H. Lee, I.-C. Hwang, Y. H. Ko, K. Kim, *Angew. Chem. Int. Ed.* **2022**, *61*, e202209326; *Angew. Chem.* **2022**, *134*, e202209326; d) S.-C. Li, L.-X. Cai, M. Hong, Q. Chen, Q.-F. Sun, *Angew. Chem. Int. Ed.* **2022**, *61*, e202204732; *Angew. Chem.* **2022**, *134*, e202204732; e) L. S. Lisboa, D. Preston, C. J. McAdam, L. J. Wright, C. G. Hartinger, J. D. Crowley, *Angew. Chem. Int. Ed.* **2022**, *61*, e202201700; *Angew. Chem.* **2022**, *134*, e202201700.

[5] a) M. Zhang, M. L. Saha, M. Wang, Z. Zhou, B. Song, C. Lu, X. Yan, X. Li, F. Huang, S. Yin, P. J. Stang, *J. Am. Chem. Soc.* **2017**, *139*, 5067–5074; b) P.-P. Jia, L. Xu, Y.-X. Hu, W.-J. Li, X.-Q. Wang, Q.-H. Ling, X. Shi, G.-Q. Yin, X. Li, H. Sun, Y. Jiang, H.-B. Yang, *J. Am. Chem. Soc.* **2021**, *143*, 399–408; c) A. Brzechwa-Chodzynska, W. Drozdz, J. Harrowfield, A. R. Stefankiewicz, *Coord. Chem. Rev.* **2021**, *434*, 213820; d) J. Zhu, Z. Yan, F. Bo˘skovic, C. Haynes, M. Kieffer, J. Greenfield, J. Wang, J. R. Nitschke, U. F. Keyser, *Chem. Sci.* **2021**, *12*, 14564–14569.

[6] a) S. Horiuchi, T. Yamaguchi, J. Tessarolo, H. Tanaka, E. Sakuda, Y. Arikawa, E. Meggers, G. H. Clever, K. Umakoshi, *Nat. Commun.* **2023**, *14*, 155; b) M. Abe, H. Yamada, T. Okawara, M. Fujitsuka, T. Majima, Y. Hisaeda, *Inorg. Chem.* **2016**, *55*, 7–9.

[7] Q. Zhang, Y. Jin, L. Ma, Y. Zhang, C. Meng, C. Duan, *Angew. Chem. Int. Ed.* **2022**, *61*, e202204918; *Angew. Chem.* **2022**, *134*, e202204918.

[8] a) J. Liu, W. Duan, J. Song, X. Guo, Z. Wang, X. Shi, J. Liang, J. Wang, P. Cheng, Y. Chen, M. J. Zaworotko, Z. Zhang, *J.*

Am. Chem. Soc. **2019**, *141*, 12064–12070; b) N. Nitta, M. Takatsuka, S.-i. Kihara, T. Hirao, T. Haino, *Angew. Chem. Int. Ed.* **2020**, *59*, 16690–16697; *Angew. Chem.* **2020**, *132*, 16833–16840.

[9] Y. Shi, J. Zhang, L. Pan, Y. Shi, G. Yu, *Nano Today* **2016**, *11*, 738–762.

[10] G. Li, J. Zhao, Z. Zhang, X. Zhao, L. Cheng, Y. Liu, Z. Guo, W. Yu, X. Yan, *Angew. Chem. Int. Ed.* **2022**, *61*, e202201101; *Angew. Chem.* **2022**, *134*, e202201101.

[11] a) C. Lu, M. Zhang, D. Tang, X. Yan, Z. Zhang, Z. Zhou, B. Song, H. Wang, X. Li, S. Yin, H. Sepehrpour, P. J. Stang, *J. Am. Chem. Soc.* **2018**, *140*, 7674–7680; b) A. Carné-Sánchez, G. A. Craig, P. Larpent, T. Hirose, M. Higuchi, S. Kitagawa, K. Matsuda, K. Urayama, S. Furukawa, *Nat. Commun.* **2018**, *9*, 2506.

[12] a) Y. Gu, E. A. Alt, H. Wang, X. Li, A. P. Willard, J. A. Johnson, *Nature* **2018**, *560*, 65–69; b) A. V. Zhukhovitskiy, M. Zhong, E. G. Keeler, V. K. Michaelis, J. E. P. Sun, M. J. A. Hore, D. J. Pochan, R. G. Griffin, A. P. Willard, J. A. Johnson, *Nat. Chem.* **2016**, *8*, 33–41; c) J. A. Foster, R. M. Parker, A. M. Belenguer, N. Kishi, S. Sutton, C. Abell, J. R. Nitschke, *J. Am. Chem. Soc.* **2015**, *137*, 9722–9729.

[13] M. Kieffer, A. M. Garcia, C. J. E. Haynes, S. Kralj, D. Iglesias, J. R. Nitschke, S. Marchesan, *Angew. Chem. Int. Ed.* **2019**, *58*, 7982–7986; *Angew. Chem.* **2019**, *131*, 8066–8070.

[14] P. Makam, E. Gazit, *Chem. Soc. Rev.* **2018**, *47*, 3406–3420.

[15] a) A. M. Garcia, D. Iglesias, E. Parisi, K. E. Styan, L. J. Waddington, C. Deganutti, R. De Zorzi, M. Grassi, M. Melchionna, A. V. Vargiu, S. Marchesan, *Chem* **2018**, *4*, 1862–1876; b) S. Marchesan, K. E. Styan, C. D. Easton, L. Waddington, A. V. Vargiu, *J. Mater. Chem. B* **2015**, *3*, 8123–8132.

[16] a) J. Dong, Y. Liu, Y. Cui, *J. Am. Chem. Soc.* **2021**, *143*, 17316–17336; b) Y. Inomata, T. Sawada, M. Fujita, *J. Am. Chem. Soc.* **2021**, *143*, 16734–16739.

[17] a) R. Zou, Q. Wang, J. Wu, J. Wu, C. Schmuck, H. Tian, *Chem. Soc. Rev.* **2015**, *44*, 5200–5219; b) S. Dey, R. Misra, A. Saseendran, S. Pahan, H. N. Gopi, *Angew. Chem. Int. Ed.* **2021**, *60*, 9863–9868; *Angew. Chem.* **2021**, *133*, 9951–9956.

[18] a) A. D. Malay, N. Miyazaki, A. Biela, S. Chakraborti, K. Majsterkiewicz, I. Stupka, C. S. Kaplan, A. Kowalczyk, B. M. A. G. Piette, G. K. A. Hochberg, D. Wu, T. P. Wrobel, A. Fineberg, M. S. Kushwah, M. Kelemen, P. Vavpetic, P. Pelicon, P. Kukura, J. L. P. Benesch, K. Iwasaki, J. G. Heddle, *Nature* **2019**, *569*, 438–442; b) K. Nishida, A. Tamura, T. W. Kang, H. Masuda, N. Yui, *J. Mater. Chem. B* **2020**, *8*, 6975–6987.

[19] A. M. Castilla, N. Ousaka, R. A. Bilbeisi, E. Valeri, T. K. Ronson, J. R. Nitschke, *J. Am. Chem. Soc.* **2013**, *135*, 17999–18006.

[20] a) N. Ousaka, J. K. Clegg, J. R. Nitschke, *Angew. Chem. Int. Ed.* **2012**, *51*, 1464–1468; *Angew. Chem.* **2012**, *124*, 1493–1497; b) A. M. Castilla, W. J. Ramsay, J. R. Nitschke, *Chem. Lett.* **2014**, *43*, 256–263.

[21] J. M. Dragna, G. Pescitelli, L. Tran, V. M. Lynch, E. V. Anslyn, L. Di Bari, *J. Am. Chem. Soc.* **2012**, *134*, 4398–4407.

[22] a) W. Xue, T. K. Ronson, Z. Lu, J. R. Nitschke, *J. Am. Chem. Soc.* **2022**, *144*, 6136–6142; b) Y. Domoto, K. Yamamoto, S. Horie, Z. Yu, M. Fujita, *Chem. Sci.* **2022**, *13*, 4372–4376.

[23] a) M. Alejandra Sequeira, M. Georgina Herrera, V. Isabel Dodero, *Phys. Chem. Chem. Phys.* **2019**, *21*, 11916–11923; b) B. K. Das, R. Samanta, S. Ahmed, B. Pramanik, *Chem. Eur. J.* **2023**, e202300312; c) C. Diaferia, E. Rosa, N. Balasco, T. Sibillano, G. Morelli, C. Giannini, L. Vitagliano, A. Accardo, *Chem. Eur. J.* **2021**, *27*, 14886–14898; d) M. C. Cringoli, S. Marchesan, *Molecules* **2023**, *28*, 4970.

[24] M. G. Herrera, F. Zamarreño, M. Costabel, H. Ritacco, A. Hütten, N. Sewald, V. I. Dodero, *Biopolymers* **2014**, *101*, 96–106.

[25] N. Sreerama, R. W. Woody, in *Methods in Enzymology, Vol. 383*, Academic Press **2004**, pp. 318–351.

[26] J. D. Hostert, C. N. Loney, N. Pramounmat, K. Yan, Z. Su, J. N. Renner, *Langmuir* **2021**, *37*, 6115–6122.

[27] J. D. A. Tyndall, B. Pfeiffer, G. Abbenante, D. P. Fairlie, *Chem. Rev.* **2005**, *105*, 793–826.

[28] R. Zhang, M. C. Stahr, M. A. Kennedy, *Proteins* **2022**, *90*, 110–122.

[29] a) D. F. Brightwell, G. Truccolo, K. Samanta, H. J. Shepherd, A. Palma, *ACS Macro Lett.* **2023**, *12*, 908–914; b) V. V. Pak, O. K. Khojimatov, A. V. Pak, S. S. Sagdullaev, L. Yun, *Int. J. Pept. Res. Ther.* **2022**, *28*, 144.

[30] S. Adorinni, S. Gentile, O. Bellotto, S. Kralj, E. Parisi, M. C. Cringoli, C. Deganutti, G. Malloci, F. Piccirilli, P. Pengo, L. Vaccari, S. Geremia, A. V. Vargiu, R. De Zorzi, S. Marchesan, *ACS Nano* **2024**, *18*, 3011–3022.

[31] N. Harada, N. Berova, *Comprehensive Chirality* **2012**, *8*, 449–477.

[32] A. P. Katsoulidis, D. Antypov, G. F. S. Whitehead, E. J. Carrington, D. J. Adams, N. G. Berry, G. R. Darling, M. S. Dyer, M. J. Rosseinsky, *Nature* **2019**, *565*, 213–217.

[33] P. Sacco, G. Baj, F. Asaro, E. Marsich, I. Donati, *Adv. Funct. Mater.* **2020**, *30*, 2001977.

[34] Y. Wang, Y. Gu, E. G. Keeler, J. V. Park, R. G. Griffin, J. A. Johnson, *Angew. Chem. Int. Ed.* **2017**, *56*, 188–192; *Angew. Chem.* **2017**, *129*, 194–198.

[35] R. D. Shannon, *Acta Crystallogr. Sect. A* **1976**, *32*, 751–767.

[36] Z.-Y. Wu, X.-X. Xu, B.-C. Hu, H.-W. Liang, Y. Lin, L.-F. Chen, S.-H. Yu, *Angew. Chem. Int. Ed.* **2015**, *54*, 8179–8183; *Angew. Chem.* **2015**, *127*, 8297–8301.

[37] Y. Jia, W. Zhang, J. Y. Do, M. Kang, C. Liu, *Chem. Eng. J.* **2020**, *402*, 126193.

[38] T.-Y. Liang, S.-J. Chan, A. S. Patra, P.-L. Hsieh, Y.-A. Chen, H.-H. Ma, M. H. Huang, *ACS Appl. Mater. Interfaces* **2021**, *13*, 11515–11523.

[39] R. M. Fogarty, R. Rowe, R. P. Matthews, M. T. Clough, C. R. Ashworth, A. Brandt, P. J. Corbett, R. G. Palgrave, E. F. Smith, R. A. Bourne, T. W. Chamberlain, P. B. J. Thompson, P. A. Hunt, K. R. J. Lovelock, *Faraday Discuss.* **2018**, *206*, 183–201.

[40] a) F. Jia, C. Liu, B. Yang, X. Zhang, H. Yi, J. Ni, S. Song, *ACS Sustainable Chem. Eng.* **2018**, *6*, 9065–9073; b) M. Madkour, Y. Abdelmonem, U. Y. Qazi, R. Javaid, S. Vadivel, *RSC Adv.* **2021**, *11*, 29433–29440.

Manuscript received: April 11, 2024
Accepted manuscript online: May 3, 2024
Version of record online: ■■, ■■

Communications

Metal-Organic Cages

M. Li, H. Zhu, S. Adorinni, W. Xue, A. Heard, A. M. Garcia, S. Kralj, J. R. Nitschke,* S. Marchesan* _____ **e202406909**

Metal Ions Trigger the Gelation of Cysteine-Containing Peptide-Appended Coordination Cages

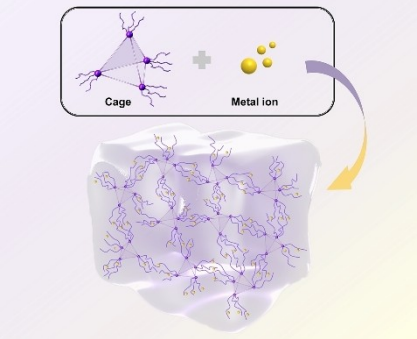

Three $Fe^{II}_4L_4$ metal-organic cages were fabricated via a L–D–L-tripeptide ligand with different sequences. The cages could form gels triggered by coordinating thiol groups of peripheral peptides around metal vertices to the second metal ion. This strategy might allow for the modular and conventional design of other recyclable and functional cage-gel materials.